

OPINION

The physics of cancer: the role of physical interactions and mechanical forces in metastasis

Denis Wirtz, Konstantinos Konstantopoulos and Peter C. Searson

Abstract | Metastasis is a complex, multistep process responsible for >90% of cancer-related deaths. In addition to genetic and external environmental factors, the physical interactions of cancer cells with their microenvironment, as well as their modulation by mechanical forces, are key determinants of the metastatic process. We reconstruct the metastatic process and describe the importance of key physical and mechanical processes at each step of the cascade. The emerging insight into these physical interactions may help to solve some long-standing questions in disease progression and may lead to new approaches to developing cancer diagnostics and therapies.

In the series of steps that comprise the metastatic process, cancer cells migrate or flow through vastly different microenvironments, including the stroma, the blood vessel endothelium, the vascular system and the tissue at a secondary site^{1,2} (FIG. 1). The ability to successfully negotiate each of these steps and advance towards the formation and growth of a secondary tumour is dependent, in part, on the physical interactions and mechanical forces between cancer cells and the microenvironment. For example, the physical interactions between a cell and the extracellular matrix — the collagen-rich scaffold on which it grows — have a key role in allowing cells to migrate from a tumour to nearby blood vessels. During intravasation and extravasation, cells must undergo large elastic deformations to penetrate endothelial cell–cell junctions. In the vascular system, the interplay between cell velocity and adhesion influences the binding of cancer cells to blood vessel walls and hence the location of sites where a secondary tumour can form and grow. A clearer understanding of the role of physical interactions and mechanical forces, and their interplay with biochemical changes, will provide new and important insights into the progression of cancer and may provide the basis for new therapeutic approaches.

Physical interactions in invasion

Following the growth of a primary tumour, the combination of continued tumour proliferation, angiogenesis, accumulated genetic transformations and activation of complex signalling pathways trigger the metastatic

cascade (FIG. 2). In particular, the detachment of carcinoma cells from the epithelium and the subsequent invasion of the underlying stroma resembles, at both the cellular and molecular levels, the well-characterized epithelial-to-mesenchymal transition (EMT) in embryogenesis³. The role of EMT in cancer metastasis is being actively explored^{4,5}. Critical to EMT is the loss of E-cadherin (an intercellular adhesion molecule) and cytokeratins, which leads to dramatic changes in the physical and mechanical properties of cells: specifically, reduced intercellular adhesion and a morphological change from cuboidal epithelial to mesenchymal⁶. One consequence of these changes is detachment from the primary tumour and the acquisition of a motile phenotype⁵. These cells also begin to express matrix metalloproteinases

(MMPs) on their surface, which promote the digestion of the laminin- and collagen IV-rich basement membrane⁷. After leaving the tumour microenvironment, motile tumour cells encounter the architecturally complex extracellular matrix (ECM), which is rich in collagen I and fibronectin⁸ (BOX 1). In the vicinity of a mammary tumour, the matrix is often stiffer than in normal tissue owing to enhanced collagen deposition⁹ and lysyl-oxidase-mediated crosslinking of the collagen fibres by tumour-associated fibroblasts¹⁰. Collagen crosslinking enhances integrin signalling as well as the bundling of individual fibres¹¹. Such changes in the physicochemical properties of the matrix can enhance cell proliferation and invasion in a positive feedback loop⁹. Whether stiffening of the stromal matrix occurs in other solid tumours, besides mammary tumours, remains to be determined. However, despite recent technological advances (TABLE 1), remarkably little is known about the molecular and physical mechanisms that drive motile cancer cells away from primary tumour and into the stromal space, especially at the subcellular level.

Motility in three dimensions. Much of what we have learned about the physical and molecular mechanisms driving normal and cancer cell motility has come from *in vitro* studies using two-dimensional (2D) substrates^{12–14}. However, the dimensionality of the system used to study cancer invasion can have a key role in dictating the mode of cell migration. This is not entirely surprising as the three-dimensional (3D) microenvironment of the ECM *in vivo* is characterized by many features, including the pore size and fibre orientation, features that are not found in conventional ECM-coated

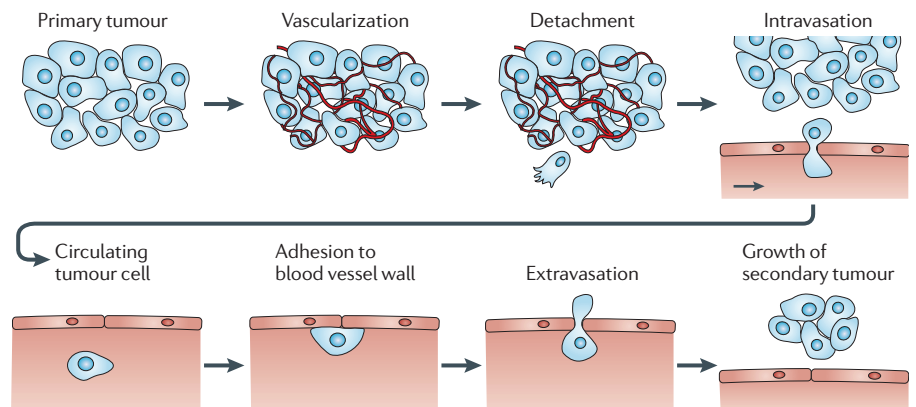


Figure 1 | The metastatic process. In this complex process, cells detach from a primary, vascularized tumour, penetrate the surrounding tissue, enter nearby blood vessels (intravasation) and circulate in the vascular system. Some of these cells eventually adhere to blood vessel walls and are able to extravasate and migrate into the local tissue, where they can form a secondary tumour.

2D substrates¹⁵. In turn, many features that are thought to be crucial for 2D motility, such as focal adhesions, stress fibres, wide lamellipodia and lamella, multiple filopodial protrusions at the leading edge and apical polarization, are either drastically reduced in size or entirely missing from motile carcinoma or sarcoma cells in a 3D matrix^{16–20}. Similarly, several cellular features that are important in 3D cell motility have little or no role in 2D cell motility, including nuclear deformation, MMP production and major reorganization of the ECM.

Recent work suggests that focal adhesions, composed of clustered integrins that physically and dynamically connect the cellular actin network to ECM fibres on 2D substrates, are altered when cells are embedded inside a 3D matrix¹⁶. Focal adhesions, which are readily visible by microscopy in human breast cancer cells, colon carcinoma cells and fibrosarcoma cells plated on 2D substrates, rapidly decrease both in size and number as a function of the distance between the cells in the matrix and the substrate that supports the matrix.

The absence of prominent focal adhesions and the associated reduction and relocalization of stress fibres that join these focal adhesions is in large part due to the 3D architecture of the ECM. In general, a cell is much larger than the diameter of the fibres of the ECM, which

are typically on the order of 100 nm. Therefore, from a cellular perspective, the collagen fibres in the ECM appear quasi-one-dimensional (1D); similarly, a human hair does not appear to have significant width and hence is quasi-1D to the eye. Focal adhesions formed on 2D substrates are typically 1–10 µm in size, much larger than the fibre diameter of the ECM^{21–23}. This finite size effect limits the size of focal adhesions and the associated clusters of integrins and focal adhesion proteins that can be formed in cells embedded in a 3D matrix. Hence, although when in 2D culture a cell is in contact with a contiguous substrate, a cell in a 3D matrix has confined local contact with quasi-1D fibres.

Nevertheless, collagen fibres in a 3D matrix could support the formation of small and highly dynamic integrin clusters, with sizes on the order of tens of nanometres and lifetimes shorter than a few seconds, which may still be crucial to 3D cell motility. Moreover, cells *in vivo* could promote the bundling of collagen fibres through the generation of contractile forces produced by cellular protrusions. Such collagen bundles would enhance the surface area available and potentially promote the formation of larger adhesions²⁴.

Actomyosin stress fibres, containing bundled actin filaments, have an important role in 2D cell motility as they provide the contractile forces required for the regulated

detachment of the rear of a cell from the substratum and establish actin flow at the leading edge of the cell^{23,25}. By contrast, cells display few stress fibres inside a 3D matrix and these are either localized to the cell cortex or radiate from the nucleus towards the plasma membrane to form pseudopodial protrusions²⁶. Inhibition of actomyosin contractility is often substantially less effective in blocking 3D cell motility than in blocking 2D cell motility²⁶, suggesting that the role of stress fibres is dependent on dimensionality^{25,27}. Hence, eliminating the apical polarization of cells in 2D culture reduces the number of focal adhesions and stress fibres, and therefore fundamentally changes the role of components such as focal adhesion proteins and proteins highly enriched in stress fibres, such as the F-actin binding proteins α -actinin, myosin II and tropomyosins.

In addition to having fewer focal adhesions and stress fibres when in a 3D matrix, cancer cells and epithelial or endothelial cells inside a 3D matrix typically do not form the characteristic wide lamellipodium and associated filopodial protrusions at the periphery. Instead, they display a limited number of pseudopodial protrusions, typically of 10–20 µm thickness, which is intermediate between a lamellipodium and filopodia¹⁶. Traction microscopy suggests that in 2D

Glossary

Amoeboid migration

A mode of three-dimensional cell migration in a matrix that involves dynamic cell-shape changes through actomyosin assembly and contractility, and adhesion to the extracellular matrix.

Epithelial-to-mesenchymal transition

(EMT). A morphological change that epithelial cells undergo, from a cubical to an elongated shape, following oncogenic transformation, which is often accompanied by loss of expression of the adhesion molecule E-cadherin. Post-EMT, cells adopt a high-motility phenotype.

Filopodia

Narrow projections of the cytoplasm extended beyond the lamellipodia of migrating cells. Filopodia are associated with the formation of nascent focal adhesions with a substratum.

Focal adhesions

Integrin clusters located at the basal surface of adherent cells that connect the extracellular matrix to the cytoskeleton through focal adhesion proteins.

Interstitial flow

Fluid flow in the extracellular matrix, often associated with lymphatic drainage of plasma back to the vascular system.

Intravital microscopy

A microscopy technique used for the observation of biological responses, such as leukocyte–endothelial cell interactions, in living tissues in real time. Translucent tissues

are commonly used, such as the mesentery or cremaster muscle, which can be easily exteriorized for microscopic observation.

Lamellipodia

Large cytoplasmic projects found primarily at the leading edge of migrating cells, particularly on two-dimensional substrates.

Mechanosensing

The ability of cells to sense and respond to changes in the mechanical compliance of a substrate. Mechanosensing is mediated by focal adhesions and the cytoskeleton in two-dimensional cell culture.

Mesenchymal migration

A mode of three-dimensional cell migration in a matrix that involves integrin-based adhesion. Mesenchymal migration occurs when the pore size of the matrix is much smaller than the cell nucleus.

Pseudopodia

Bulges of constantly changing shape observed in the plasma membrane of migrating cells during amoeboid migration on two-dimensional substrates and mesenchymal migration through three-dimensional matrices.

Shear rate

The relative velocities of adjacent layers of fluid under shear force in conditions of laminar flow.

Shear stress

The magnitude of the tangential force applied onto the surface of an object per unit area. Shear stress is expressed in units of force per unit area (Newtons m⁻² in metres kilograms seconds (MKS) units or dynes cm⁻² in centimetres grams seconds (CGS) units).

Stiffness

(Also known as elasticity or elastic modulus). A measure of the ability of a material to resist shear forces similarly to a solid. Rubber is elastic and shows little viscosity. A crosslinked collagen matrix is elastic, but not viscous as it does not flow. The cytoplasm of cells is both elastic and viscous (viscoelastic) depending on the rate of deformation.

Stress fibres

Contractile actin filament bundles that contain myosin II, which serves both as an F-actin bundling protein and as a force generator. Stress fibres terminate at focal adhesions at the basal surface of cells on substrates.

Surface tangential velocity

The velocity at the surface of a spinning object.

Translational velocity

The velocity of an object in space.

Viscosity

A measure of the ability of a material to flow like a liquid. Water, glycerol and honey are liquids of increasing viscosity; they are only viscous and show no elasticity.

culture, a lamellipodium actively pulls the rest of the cell through nascent focal adhesions positioned at the edge of the lamellipodium²⁸. By contrast, 3D traction microscopy reveals that cells inside a 3D matrix never push the surrounding matrix and only pull on surrounding fibres^{26,29}. Substantial matrix traction only occurs in the vicinity of productive pseudopodial protrusions, which typically number between only one and five per cell at any time²⁶. Interestingly, in a 3D matrix, pseudopodial protrusions pull with approximately equal forces at the leading and trailing cell edges. However, the timing of release of the pseudopodia from the collagen fibres is asymmetric, often creating a defect in the matrix in the wake of the cell. These results suggest a model for 3D cancer cell motility in which pseudopodial protrusions at the trailing edge of the cell release first, pulling the rear of the cell forwards. The partial digestion of the ECM in the wake of the cell results in biased motion, analogous to a biased ratchet. This defect does not allow the cell to retrace the tunnel formed during migration and, therefore, promotes highly persistent migration in a 3D matrix, compared to less persistent migration of the same cell on a 2D substrate²⁰.

Pseudopodia also have a probing role in 3D matrices but are of no functional importance on 2D substrates, where the extracellular environment is compositionally and topologically uniform. The interplay between the growth of pseudopodia along the quasi-1D tracks provided by the collagen fibres, the magnitude of traction and local digestion mediated by MMPs has not been determined but is likely to be fundamentally different from the 2D case given the different

shapes of membrane protrusions and the crucial importance of MMPs in 3D cell motility. As cellular traction on collagen fibres may activate MMPs³⁰, the interplay among pulling by cell protrusions, MMP activity and net cell migration is likely to occur within a feedback loop.

Pseudopodial protrusion activity in 3D matrices is readily modulated by focal adhesion components. For example, the scaffolding protein p130CAS mediates a high number and high growth rate of protrusions, whereas the mechanosensing protein zyxin represses protrusion activity and diminishes the rate of protrusion growth along collagen fibres. A recent study¹⁶ showed that the number of protrusions per unit time as well as the growth rate of protrusions, as modulated by focal adhesion proteins, correlated strongly with tumour cell motility in 3D matrices, a correlation shared by sarcoma and carcinoma cells. For instance, the migration speed of p130CAS- and zyxin-depleted cells correlated with the number of protrusions generated per unit time by these cells in 3D matrices¹⁶. However, whereas p130CAS-depleted cells moved more slowly (and zyxin-depleted cells more rapidly) than control cells in 3D matrices, these depleted cells displayed the opposite motility phenotypes on flat substrates. Importantly, modulation of 3D cell motility by the depletion of specific focal adhesion proteins does not correlate with changes in motility on 2D substrates. For example, vinculin-depleted cells move at a similar speed to control cells on flat substrates, whereas they move faster than control cells inside a 3D matrix¹⁶. Therefore, the role of focal adhesion proteins in 2D cell motility is not predictive of

their role in motility in more physiologically relevant 3D matrices. Such results suggest that high-throughput pharmacological screens for drugs that limit motility on 2D substrates could be misleading. Moreover, although the rate of filopodial protrusion does not seem to correlate with 2D cell speed, the rate of pseudopodial protrusion correlates with 3D cell speed¹⁶. This suggests that protrusion dynamics is not required per se for effective 2D motility, but may be crucial in establishing 3D motility.

Many features observed *in vivo* by intravital microscopy³¹ have been recapitulated in 3D matrix constructs, including the highly persistent migration of single cells away from tumours, the role of actomyosin contractility in collective migration to lymphatic vessels and the crucial role of MMPs in cancer cell dispersion from a primary tumour site. Nevertheless much more needs to be done to validate 3D models for *in vitro* cancer studies.

Intravital imaging of mammary tumours in mice suggests that only a small number of cells leave the primary tumour sites, and that they undergo highly directed migration away from the tumour by travelling along collagen fibres^{1,32}. Intravital microscopy of GFP-labelled breast cancer cells in mice suggests that these cells migrate as single cells towards blood capillaries, and as multicellular clusters preferentially towards lymphatic vessels³³. Such collective migration requires the suppression of actomyosin contractility at intercellular adhesions, which is mediated by discoidin domain receptor family, member 1 (DDR1) and the polarity regulators PAR3 and PAR6 (REF. 34). To establish the *in vivo* relevance of *in vitro* 3D matrix-based models, it will be important to confirm the role of focal adhesion proteins in cancer cell motility (suggested by the *in vitro* 3D assays described above) using intravital microscopy.

Signalling and motility in cancer cells. The role of other prominent proteins that normally localize to the lamellipodium and filopodia of cells in 3D matrices is largely unknown. These proteins include those that constitute the F-actin nucleating ARP2/3 complex and its activators neural Wiskott–Aldrich syndrome protein (NWASP), Wiskott–Aldrich syndrome protein family, member 1 (WASF1; also known as WAVE1), WASF2 and WASF3 (also known as SCAR3), the expression of which correlates with poor clinical outcomes in several types of cancer^{35,36}. Expression of the F-actin bundling protein fascin, which localizes to filopodia in 2D cell cultures, also correlates with poor clinical outcomes

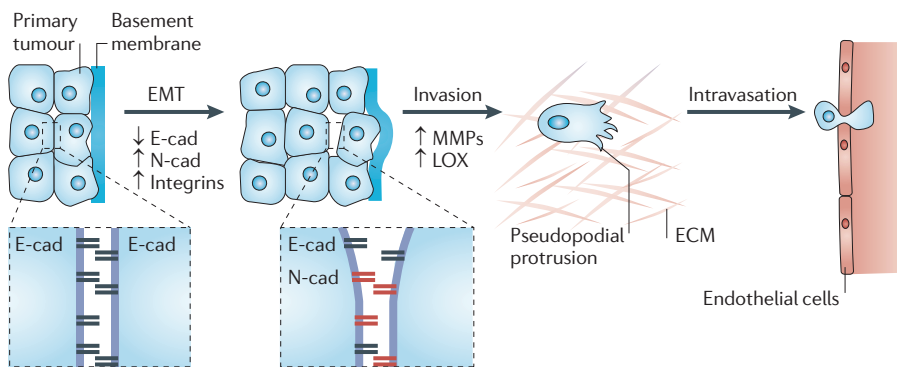


Figure 2 | The physics of invasion and intravasation. The epithelial-to-mesenchymal transition (EMT) is associated with a loss of adhesion through downregulation of E-cadherin (E-cad) and a change in morphology. Invasion by tumour cells of the surrounding tissue and subsequent motion is dictated by the physicochemical properties of the extracellular matrix (ECM). By squeezing between blood vessel endothelial cells, tumour cells can enter the vascular system. All of these steps involve physicochemical processes, such as adhesion and deformation, that are dependent on the local environment. LOX, lysyl oxidase; MMPs, matrix metalloproteinases; N-cad, N-cadherin.

Box 1 | The extracellular matrix

The extracellular matrix (ECM) is a complex composite material consisting of proteoglycan hydrogel coupled to an assembly of crosslinked collagen fibres that are typically 100 nm or less in diameter¹¹⁶. The unique three-dimensional architecture provides structural support and also allows sensing and transduction of biochemical and mechanical signals to cells¹¹⁷. The properties of the ECM are tissue-dependent: for example, the elasticity of ECM varies from less than 1 kPa in the brain to 100 kPa in skeletal tissues¹¹⁸. The interstitial space in the ECM is occupied by fluid that is usually in motion and provides a dynamic environment for cells⁶⁷. The permeability of the ECM is dependent on its composition and structure. The development of *in vitro* models of ECM that can mimic tissue-specific physicochemical properties, molecular composition, elasticity, pore size and local fibre orientation will be crucial to further advance our understanding of cancer cell motility in three dimensions and how this relates to migration *in vivo*.

in patients with breast cancer³⁷. In addition, the tumour suppressor protein PTEN³⁸ has been shown to localize at the trailing edge of migrating cells³⁹. Therefore, the development of therapeutic approaches targeting mediators of cell motility and invasion will require a greater understanding of the role of these proteins in the more physiological environment of a 3D matrix or *in vivo*.

MMP inhibition or depletion in carcinoma and fibrosarcoma cells has been observed to switch the mode of migration from a predominantly integrin-based motility to a faster amoeboid migration mode⁴⁰. By contrast, inhibition of the master mediators of actomyosin contractility, ROCK and RHO, forces the adoption of a mesenchymal migration mode in cells with an intrinsic amoeboid shape when embedded in Matrigel⁴¹. These observations provide a possible explanation for the failed clinical trials of MMP inhibitors. However, these *in vitro* studies made use of pepsin-extracted collagen I and commercially available Matrigel, which are both largely uncrosslinked. In particular, pepsin extraction of collagen I results in larger pores during gelation¹⁵ that are permissive for amoeboid migration. The motility of cancer cells in crosslinked collagen gels crucially requires MMPs, primarily MMP14 (also known as MT1-MMP)^{8,15,42}. These seemingly contradictory results can be reconciled if MMP function depends on the collagen matrix microstructure, including the collagen concentration and crosslinking density. MMP inhibition would be effective in reducing cancer cell motility in highly crosslinked and/or concentrated regions of the matrix, but would be ineffective for poorly crosslinked and/or low density regions. Interestingly, recent results suggest that mechanical load can dramatically increase the rate of collagen proteolysis by MMP14 (REF. 43). Moreover, combined inhibition of MMPs and actomyosin contractility reduces cell migration more effectively than separate inhibition of MMPs or contractility²⁶. These results suggest an

important functional interplay between cellular contractility and local MMP-mediated collagen digestion that drives cell migration in 3D matrices.

There is accumulating evidence that the physical properties of the stroma have a crucial role in tumour initiation, progression and metastasis through interplay between physical forces and biochemical signals. For example, the stiffness of the stromal matrix and degree of orientation of matrix fibres near primary tumour sites strongly correlate with worse clinical outcomes. Both *in vitro* and *in vivo*, these two microstructural parameters alone greatly enhance cell proliferation and motility^{9,18,44–46}.

The role of cell mechanics in intravasation

During entry into, and exit from, the vascular system, tumour cells undergo dramatic shape changes, driven by cytoskeletal remodelling, that enable them to penetrate endothelial cell–cell junctions. The cytoplasm is a complex composite system that behaves like an elastic material (such as rubber) at high deformation rates but more like a viscous material (such as ketchup) that exhibits a yield stress at low deformation rates⁴⁷. Elasticity reflects the ability of the cytoplasm to rebound following the application of a force, whereas viscosity measures the ability of the cytoplasm to undergo flow under external shear. However, as MMP-mediated digestion of the matrix seems to be only partial, the rate-limiting step in the migration of cancer cells within a matrix or across an endothelium may be the deformation of the interphase nucleus, which is the largest organelle in the cell⁴⁸ and is approximately ten times stiffer than the cytoplasm^{49,50}. The elasticity of the nucleus seems to be determined by the nuclear lamina underlying the nuclear envelope⁴⁹ and by both chromatin organization⁵¹ and linkers of the nucleus and cytoskeleton (LINC) complexes^{52–55}. LINC complexes are protein assemblies that span the nuclear envelope and mediate physical

connections between the nuclear lamina and the cytoskeleton⁵². These connections are mediated by interactions between SUN domain-containing proteins (including SUN1 and SUN2) and Klarsicht homology (KASH) domain-containing proteins at the outer nuclear membrane (including the nesprin 2 giant isoform and nesprin 3, which can bind actin directly or indirectly)^{56–58}. Indeed, depletion of LINC complex components, including nesprins and SUN proteins, leads to nuclear shape defects and an associated softening of the nucleus and the cytoplasm⁵⁹. The nuclear lamina and LINC complex molecules have crucial roles in collective 2D migration^{54,55}; however, their role in 3D motility remains to be explored. Mutations that occur in nesprins and lamin A/C that have been found in breast cancer⁴⁰ could cause changes in LINC-mediated connections between the nucleus and cytoskeleton and, in turn, affect cancer cell 3D motility and invasiveness.

Biophysical measurements that compare the mechanical properties of normal and cancer cells have consistently shown that cancer cells are softer than normal cells and that this cellular compliance correlates with an increased metastatic potential^{60,61}. In cancer cells, a softer cytoplasm correlates with a less-organized cytoskeleton. However, softening of the cytoskeleton has yet to be verified *in vivo* or in a 3D matrix in the presence and absence of interstitial flow. This is important as the physical properties of the environment, such as ECM stiffness⁶² and dimensionality^{63–65} and the presence of interstitial flow, regulate cell mechanics⁶⁶. The development of new methods, such as particle-tracking microrheology⁴⁷, will allow these measurements to be carried out in animal models, enabling a direct test of the hypothesis that cancer cells display lower stiffness than non-transformed cells. Such a finding could be used as a biophysical diagnostic marker of disease and metastatic potential⁶⁰. We note that the reason why cancer cells may be softer than non-transformed cells is not currently known.

Migration through a 3D matrix and penetration through an endothelium is likely to require optimal mechanical properties: if they are too stiff or too soft, cells cannot deform the highly crosslinked collagen fibres of the matrix to migrate efficiently. However, single-cell measurements have consistently revealed that individual cells of a particular cell type are usually heterogeneous and display a wide range of mechanical properties. This suggests that cells with the optimal mechanical properties for invasion and intravasation into blood vessels are

Table 1 | Tools for the study of the physics of cancer

Tool or technique	Application	Refs
Cellular adhesion and migration		
Single-molecule force spectroscopy	Measurements of cell–matrix and cell–cell adhesion at single-molecule resolution; measurement of single ligand–receptor binding <i>in vivo</i>	120–125
Flow chamber assays	Measurement of global cell–matrix adhesion	103,126–128
Adhesive micropatterns	Control of cell and nuclear shape and size; control of axis of cell division; high-throughput drug testing	129–133
Adhesive nanopatterns	Control of subcellular adhesion; integrin clustering	21
Programmed subcellular release	Controlled localized detachment of cells from substrates	134–136
Deformable pillars	Measurement of local traction forces generated by cells; application of localized forces to the basal surface of cells	137,138
3D traction microscopy	Measurement of cell-induced 3D matrix remodelling	26
2D traction microscopy	Measurement of forces generated by cells on 2D substrates	139
Galvanotaxis	Measurement of the influence of electric field on motility	140,141
Controlled cellular polarization		
Flow chambers	Measurements of cell polarization induced by flow and mechanotransduction	142,143
Wound-healing	Measurements of migration and polarization during collective cell migration	144
Single-cell motility	Measurement of motility parameters for cells on substrates and in 3D matrices	16
Micropatterns for wound-healing	Measurement and control of cell polarization during collective cell migration	145–147
Cellular and nuclear mechanics		
Atomic force microscopy	Measurement of cellular and single-molecule mechanics; imaging of cells at the nanoscale; application of controlled forces to the apical surface of cells	45,62,148
Particle tracking microrheology	Measurement of intracellular, nuclear and extracellular matrix mechanics <i>in vitro</i> and <i>in vivo</i>	50,63,149
Magnetic/optical tweezers	Measurement of cellular and subcellular mechanics; application of localized forces at the cell surface and in the cytoplasm	61,150
Calibrated microneedles	Application of localized forces to the apical surface of cells and measurement of cell mechanotransduction	151–153
Laser ablation	Ablation of cytoskeletal fibres	154–156
Micropipette suction	Measurement of cellular and nuclear mechanics	49,157,158
Controlled microenvironment		
Substrates of controlled compliance	Measurement of cellular mechanosensing; testing of the role of microenvironment compliance on cellular functions	159,160
Substrates of controlled nanotopography	Testing the role of local topography on cell functions	161–163
Stretchable substrates	Measurement of subcellular and nuclear mechanotransduction	59,164
Biomimetic matrices	3D matrices of controlled pore size, compliance and distance between ligands	165
Adhesive micropatterns	Control of the dimensionality of the microenvironment (1D versus 2D); control of cell shape and size	20,131,132
Confining microchannels	Measurement of cell motility in confined spaces	166
Microfluidic devices	Control and measurement of cell chemotaxis and durotaxis; cell sorting; high-throughput molecular detection	61,167–170
Imaging		
Multiphoton laser scanning microscopy	Real-time imaging of individual cells and extracellular matrix <i>in vivo</i>	31,73,171,172
Fluorescence recovery after photobleaching (FRAP)	Measurement of the subcellular diffusion of molecules	173,174
Fluorescence loss in photobleaching (FLIP)	Measurement of the net transport of molecules in the cytoplasm	123,173,174
Fluorescence resonance energy transfer (FRET)	Protein localization and activity in live cells	175,176
Fluorescence lifetime imaging (FLIM)	Fluorescence imaging in thick samples	177
Fluorescence correlation spectroscopy	Dynamics of molecules in live cells	178,179
Photoactivation	Activation of proteins; ultraresolution microscopy	180–182

1D, one-dimensional; 2D, two-dimensional; 3D, three-dimensional.

likely to preserve this phenotype over several generations. If mechanical properties are determined randomly on cell division, the broad distribution of mechanical properties implies that migration and intravasation would be unlikely events. Therefore, an important question is whether the physical attributes of cancer cells, such as stiffness, are passed on from generation to generation. If these physical properties are inherited, then it may be possible to alter them, either through pharmacological inhibition or activation of proteins affecting cell mechanics, so that they are not optimal for stromal invasion and intravasation.

Different optimal mechanical properties are probably required for each step of the metastatic cascade. For example, the optimal mechanical properties for invasion into the stromal matrix near the primary tumour site could be different from the mechanical properties of cells that have optimal (efficient) intravasation. Hence the mechanical properties of cancer cells might dynamically change during the metastatic process to successfully survive the harsh and changing environment of blood vessels, lymphatic vessels and the stromal space. These differences in mechanical properties might also be modulated by biochemical gradients⁵⁰, interstitial flows⁶⁷ and endogenous electric fields⁶⁸.

Shear stress and the circulatory system

During their transit through the circulatory system, tumour cells are subjected to haemodynamic forces, immunological stress and collisions with host cells, such as blood cells and the endothelial cells lining the vessel wall. All of these stresses could affect cell survival and the ability to establish metastatic foci. Only circulating tumour cells (CTCs) that overcome or even exploit the effects of fluid shear (see below) and immunosurveillance will adhere to the vascular endothelium of distant organs, exit the circulation and successfully enter these tissues. A tiny fraction of CTCs survive to generate metastases; most CTCs die or remain dormant⁶⁹.

On entering the circulatory system, the trajectory or path of a tumour cell is influenced by a number of physical and mechanical parameters: the pattern of blood flow, the diameter of the blood vessels and the complex interplay between shear flow and intercellular adhesion that leads to the arrest of cell movement in larger vessels. Shear stress (τ) arises between adjacent layers of fluid (in this case blood) of viscosity (μ) moving at different velocities. The velocity of a fluid in a cylindrical tube

is maximum at the centre and zero at the cylinder walls, and the relative velocities of parallel adjacent layers of fluid in laminar flow define the shear rate ($dy/dt \equiv \dot{\gamma}$) where γ is the amplitude of deformation and t is the time elapsed. Shear stress is defined by the product of fluid viscosity and shear rate, and has units of force per unit area (Newtons per square metre (N m^{-2}) or dynes per square centimetre (dyn cm^{-2})).

The viscosity of blood is about 4 centipoise (cP), which is considerably greater than the viscosity of water (0.7 cP at 37°C), primarily owing to the presence of red blood cells. At shear rates greater than 100 s^{-1} , blood is considered a Newtonian fluid, implying that the shear stress increases linearly with shear rate. The normal time-averaged levels of shear stress vary between 1–4 dyn cm^{-2} in the venous circulation and 4–30 dyn cm^{-2} in the arterial circulation⁷⁰. The maximum shear stress is experienced at the vessel wall. The mean blood velocity (v_{av}) in arteries for a vessel of diameter $d = 4 \text{ mm}$ is 0.45 m s^{-1} , whereas $v_{\text{av}} = 0.1 \text{ m s}^{-1}$ in a 5 mm vein. The corresponding shear rates ($dy/dt = 8v_{\text{av}}/d$) are 900 s^{-1} in arteries and 160 s^{-1} in veins.

The interstitial fluid velocity in other tissues, such as cartilage and bone subjected to mechanical loading during daily activity, induces varying levels of fluid shear stress up to 30 dyn cm^{-2} (REFS 2,71). Cells in the gastrointestinal tract are also constantly subjected to peristalsis and fluid shear stresses up to 30 dyn cm^{-2} . Renal epithelial cells normally sense stresses up to 0.5 dyn cm^{-2} (REF. 72), which are significantly increased under pathological conditions such as hypertension.

Shear flow influences the translational and rotational motion of CTCs (see the next section) and hence determines the orientation and time constant associated with receptor–ligand interactions that lead to adhesion. Shear flow may also induce deformation of CTCs and margination towards the vessel

walls. However, the magnitude of these effects and their influence on occlusion and adhesion remain to be determined. Surprisingly, little is known about the effects of shear flow on the viability and proliferation of CTCs.

Extravasation of circulating tumour cells

For a circulating tumour cell to exit the circulatory system, it must first bind to a blood vessel wall. There are two mechanisms of arrest, physical occlusion and cell adhesion; the relative prevalence of these mechanisms depends on the local blood vessel diameter (FIG. 3).

Physical occlusion. If a circulating tumour cell enters a vessel whose diameter is less than the circulating tumour cell ($d_{\text{vessel}} < d_{\text{cell}}$), then arrest can occur by mechanical trapping (physical occlusion). As circulating tumour cells of epithelial origin are typically $>10 \mu\text{m}$ in size, physical occlusion occurs in small vessels or capillaries of $<10 \mu\text{m}$. Arrest at branches in blood vessels in the brain, with subsequent extravasation and metastasis formation, has been observed by intravital microscopy in a mouse model⁷³.

Adhesion. Extravasation of a tumour cell from a large blood vessel ($d_{\text{cell}} < d_{\text{vessel}}$) requires the adhesion of the cell to the vessel wall through the formation of specific bonds. The probability (P) of arrest at a large vessel can be written as $P \propto ft$, where f is the collision frequency between membrane-bound receptors and endothelial ligands and t is the residence time⁷⁴. The residence time is dependent on the shear force exerted on the cell and the adhesive forces associated with ligand–receptor pairs between the circulating tumour cell and the endothelial cells of the blood vessel wall. Increasing fluid shear is expected to increase the collision frequency with the endothelium but decrease the residence time of receptor–ligand pairs.

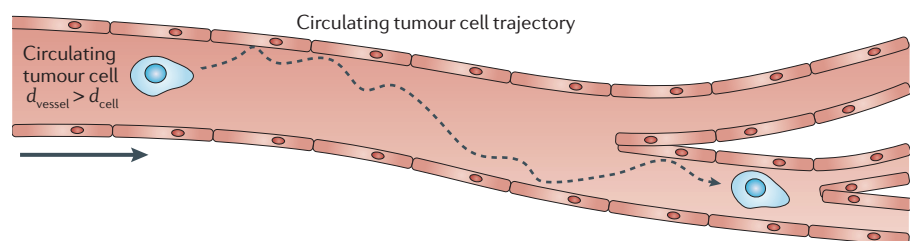


Figure 3 | Arrest of circulating tumour cells. Tumour cells with a diameter (d_{cell}) less than the diameter of the blood vessel wall (d_{vessel}) will follow a trajectory that is determined by the local flow pattern and by collisions with host cells and blood vessel walls. Collisions with a blood vessel wall may lead to arrest. Tumour cells with diameter greater than the diameter of a blood vessel will be arrested owing to mechanical trapping (physical occlusion).

A cell moving along a vessel wall has both translational and tangential (angular) velocity (BOX 2). The translational velocity of a cell is always larger than the surface tangential velocity, resulting in a slipping motion relative to the stationary blood vessel wall. This slipping motion increases the encounter rate between a single receptor on a CTC and ligands on the vessel wall⁷⁵. For a cell undergoing rotational motion, the rotation brings successive receptors on the CTC surface into contact with ligands on the vessel wall. The total adhesion strength depends in non-trivial ways on the tensile strength of the individual receptor–ligand bond and the number of the involved receptor–ligand pairs. For example, cell adhesion or cell aggregation assays have been used to quantify global cell–cell adhesion^{76,77}. However, these assays linearly extrapolate multiple-bond avidity to evaluate receptor–ligand affinity, an oversimplification that neglects possible cooperative effects. The development of sophisticated biophysical tools for measuring the kinetic and micromechanical properties of single ligand–receptor bonds have allowed single-molecule affinity to be distinguished from multi-molecular avidity^{78,79}.

The probability of arrest, leading to extravasation, is expected to be maximum at intermediate values of shear stress. The kinetic (ON and OFF rates) and micro-mechanical (tensile strength) properties of a single receptor–ligand bond dictate whether a bond will form at a prescribed shear stress level as well as the macroscopic pattern of cell adhesion (FIG. 4). For instance, the initiation of receptor-mediated cell adhesion under shear stress requires: a relatively fast ON rate, which allows receptor–ligand binding at relatively short interaction (encounter) timescales; sufficient tensile strength to resist the dispersive hydrodynamic force; and a relatively slow OFF rate, which will provide adequate bond lifetime, thereby facilitating the formation of additional bonds. Receptor–ligand pairs — such as the selectins and their ligands discussed below — that exhibit high tensile strengths, fast ON rates and relatively fast OFF rates can initiate binding under shear stress and mediate transient rolling interactions. Molecules with slower ON rates, such as integrins, can engage only after selectin-mediated cell binding or, in the absence of selectin-dependent interactions, at a very low shear stress. Integrin clustering is responsible for the multi-bond, firm adhesion of cells onto

Box 2 | Fluid shear stress and slipping velocity

For a moving spherical object with translational velocity (v_{cell}), the angular velocity (ω) describes the rate of spinning about its rotational axis, and the surface tangential velocity (v_{tg}) describes the velocity at the surface. For example, the translational velocity of the earth (about 30 km s^{-1}) results in one rotation around the sun in one year. The angular velocity results in one rotation around the polar axis in one day (about 2π radians per day) and is independent of longitude. The surface tangential velocity is highest at the equator and is about 465 m s^{-1} . For a spherical object in contact with a surface in a low viscosity fluid, such as air, the translational velocity is synchronized with the angular velocity. This situation can be envisioned as a ball rolling along the floor where $v_{\text{tg}}/v_{\text{cell}} = 1$. Numerical solutions of $v_{\text{tg}}/v_{\text{cell}}$ (REF. 119) show that for a spherical cell touching the surface in a viscous fluid, $v_{\text{tg}}/v_{\text{cell}} = 0.57$. Therefore, both translational motion and rotation along a vessel wall contribute to receptor–ligand interactions. In the absence of a slipping motion, each cell receptor can only interact with a limited number of immobilized counter-receptors located within its reactive zone. Binding occurs only when the separation distance between a receptor and a ligand is sufficiently small, within the reactive radius around a receptor. Thus, when a free ligand is brought inside this reactive zone, the complex will react. By contrast, when a cell moves with a finite slipping velocity, each cell receptor can potentially bind to any counter receptor present within its reactive zone. Thus, the slipping velocity has been reported to enhance the receptor–ligand encounter rate⁷⁵.

surfaces⁸⁰. Thus, integrins are involved in the dissemination of tumour cells, and may also control angiogenesis and metastatic growth⁸¹.

The nature of receptor–ligand interactions in the adhesion of CTCs. Evidence suggests that CTCs may escape immune surveillance and promote their egress from the circulatory system by associating with platelets. Direct evidence for the role of platelets in metastasis comes from studies in a mouse model showing the inhibition of metastasis by either pharmacological⁸² or genetic⁸³ depletion of platelets, and the restoration of metastatic potential by platelet infusion⁸⁴. It is thought that by forming heterotypic adhesive clusters with CTCs, platelets mask and protect CTCs from immune-mediated mechanisms of clearance^{85,86}. Platelets may also facilitate tumour cell adhesion to the vessel wall^{87–89} (FIG. 4) and release an array of bioactive compounds such as vascular endothelial growth factor (VEGF) at points of attachment to the endothelium, thereby promoting vascular hyperpermeability and extravasation⁹⁰. After tumour cells have exited the circulation, factors secreted from activated platelets can induce angiogenesis and stimulate growth at the metastatic site⁹¹. CTCs may also hijack polymorphonuclear leukocytes (PMNs) for arrest in the endothelium of distant organs. Microscopy studies have shown PMNs in close association with metastatic tumour cells during tumour cell arrest and extravasation *in vivo*⁹².

CTCs may also mimic the behaviour of neutrophils by directly binding to the vascular endothelium through selectin-mediated tethering and by cell rolling followed by strong adhesion^{87,93}. Indeed,

P-, L- and E-selectins facilitate cancer metastasis and tumour cell arrest in the microvasculature by mediating specific interactions between selectin-expressing host cells and ligands on tumour cells. The most direct evidence for the involvement of P-selectin (which is present on activated platelets and the endothelium) in the metastatic process is the marked inhibition of metastasis in P-selectin-knockout mice compared to wild-type controls in a colon carcinoma xenograft model^{94,95}. Similarly, mice deficient in L-selectin, which is expressed only by leukocytes, have reduced levels of metastasis⁹⁵. The extent of metastasis is further reduced in P- and L-selectin double-deficient mice⁹⁵, thereby suggesting that P- and L-selectins have synergistic effects in the facilitation of metastatic spread. It is thought that tumour cells can form multicellular complexes with platelets and leukocytes (via P- and L-selectin-dependent mechanisms^{96,97}, respectively). These multicellular complexes can then arrest in the microvasculature of distant organs, and can eventually extravasate and establish metastatic colonies. Interestingly, leukocyte L-selectin can also enhance metastasis by interacting with endothelial L-selectin ligands that are induced adjacent to established intravascular colon carcinoma cell emboli⁹⁸. Endothelial E-selectin has also been shown to support metastatic spread *in vivo*^{99,100}.

Selectins bind to sialofucosylated oligosaccharides, such as sialyl Lewis^x (sLe^x) and its isomer sLe^a, which are present mainly on cell surface glycoproteins. Various metastatic tumour cells, such as colon and pancreatic carcinoma cells, express sialofucosylated glycoproteins such as

CD44 variant isoforms, carcinoembryonic antigen (CEA) and podocalyxin (PODXL), all of which are recognized by selectins^{101–103}. As overexpression of these moieties on tumour cells correlates with poor prognosis and tumour progression¹⁰⁴, it appears that selectin-mediated adhesion to these sialofucosylated target molecules on tumour cells may represent an important determinant for metastatic spread. Thus, the intravascular phase of the metastatic process represents a key step in which therapeutic intervention may be successful¹⁰⁵. We note that additional molecules, such as glycoprotein Iba (GPIIb) and GPVI^{106,107}, integrins and their counter receptors, intercellular adhesion molecule 1 (ICAM1) and vascular cell adhesion molecule 1 (VCAM1), may be involved in tumour cell–host cell interactions¹⁰⁴ (FIG. 4).

The location of metastatic sites. The location of metastatic sites with respect to a primary tumour has been the subject of intense investigations for many years^{2,108–110}. Analysis of autopsy data revealed that metastatic sites are not colonized randomly^{108,111}. Although primary tumours are found to metastasize to many different sites, there is a higher probability of metastasis at certain sites. For example, prostate cancer tends to metastasize to bone marrow and the liver, whereas breast cancer tends to metastasize to bone marrow and the lungs. Pancreatic cancer and colon cancer tend to metastasize to the liver and the lungs.

The patterns of metastasis have been explained in terms of two hypotheses. The ‘seed and soil’ hypothesis states that a tumour cell will metastasize to a site where the local microenvironment is favourable¹¹², just as a seed released by a plant will only grow if it lands at a site where the soil is fertile. The ‘mechanical’ hypothesis states that metastasis is likely to occur at sites based on the pattern of blood flow¹⁰⁸. Both blood flow (the mechanical hypothesis) and local microenvironment (the seed and soil hypothesis) are thought to have complementary roles in influencing the location of a metastatic site^{2,108}.

Based on the preceding discussion of the arrest of circulating tumour cells, we can elaborate on the physics of the location of metastatic sites. Blood is circulated from most organs to the heart and then the lungs by the venous system, and is subsequently returned to the heart and circulated to the organs by the arterial system. The organ capillary beds are characterized by a network of small blood vessels. If a tumour cell encounters a capillary

of diameter smaller than the size of the cell ($d_{\text{cell}} > d_{\text{vessel}}$) then the probability of cell trapping by physical occlusion at that site is very high. For a metastasis to occur, the tumour cell must still extravasate and colonize the local tissue. In one study, more than 50% of metastases could be explained by the blood flow pattern between the primary and secondary site¹¹¹. As cell trapping, extravasation and colonization occur in series, we can speculate that the probability of a metastasis occurring at a specific site in accordance with the mechanical hypothesis can be expressed as $P \propto P_t \cdot P_{e,i} \cdot P_{c,i}$, where P_t is the probability of encountering a vessel with diameter less than the cell diameter, $P_{e,i}$ is the probability of extravasation at that site and $P_{c,i}$ is the probability of colonization. The probability of extravasation and colonization is expected to be dependent on the local microenvironment.

Every collision between a circulating tumour cell and a blood vessel wall, where $d_{\text{cell}} < d_{\text{vessel}}$, has the potential to result in adhesion. If the residence time is sufficiently long, then the tumour cell may adhere to the blood vessel wall and then extravasate. The probability that the residence time is sufficiently long for eventual extravasation to occur is related to the local shear stress. A further complexity is that the expression levels for adhesion proteins are different in different organs and hence the strength of the receptor–ligand adhesion may also be organ-specific¹¹³. For the seed and soil hypothesis, we write the probability of metastasis occurring at a specific site i as $P_i \propto P_{a,i} \cdot P_{e,i} \cdot P_{c,i}$, where $P_{a,i}$ is the probability that a collision at site i leads to adhesion and $P_{e,i}$ and $P_{c,i}$ are the same as defined above. From these considerations it is evident that the probability of metastasis occurring in a specific organ in both the

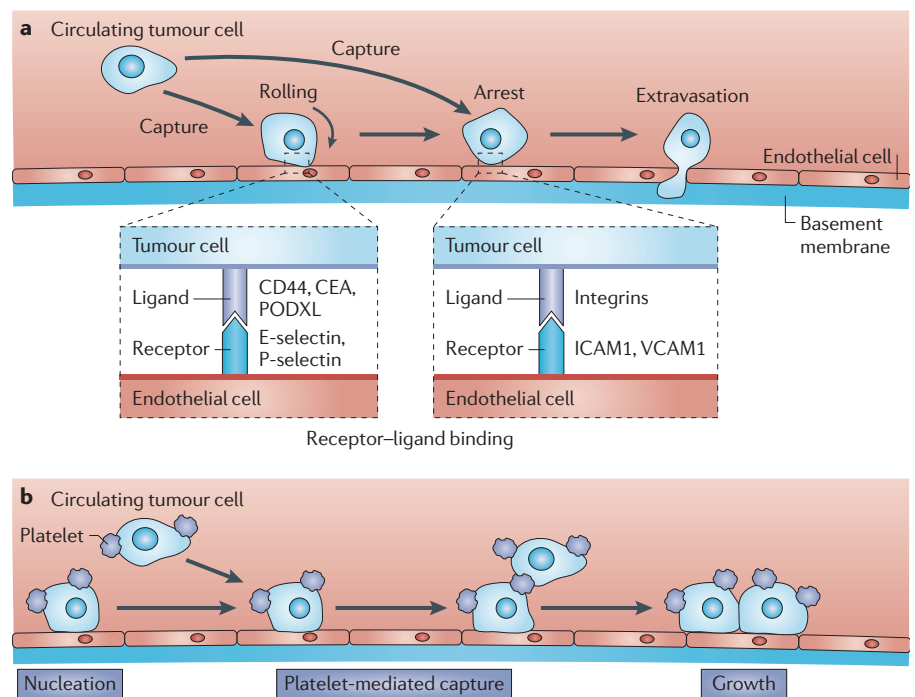


Figure 4 | Capture and arrest of circulating tumour cells. **a** | A collision between a cell and a vessel wall may lead to transient and/or persistent (firm) adhesion as a result of ligand–receptor interactions. Transient adhesion is characterized by weaker bonds involving ligands such as CD44, carcinoembryonic antigen (CEA) or podocalyxin (PODXL) binding with selectin receptors. Persistent adhesion either follows transient binding or is initiated at very low shear stress and involves interactions between integrins and their receptors, such as intercellular adhesion molecule 1 (ICAM1) and vascular cell adhesion molecule 1 (VCAM1). For consistency we designate the adhesion molecules on the surface of endothelial cells as receptors and the interacting molecules on the circulating tumour cells as ligands. We note that in the literature, integrins participating in receptor–ligand pairs are usually identified as receptors. **b** | The association of tumour cells with platelets may enhance arrest through platelet-mediated capture, a process analogous to nucleation and growth. The growth process is achieved by a platelet-bridging mechanism, whereby platelets adhere to an endothelium-bound carcinoma cell serve as a ‘nucleus’ to capture free-flowing cells that subsequently attach to the blood vessel wall downstream or next to the already adherent cell. This nucleation mechanism, which is primarily dependent on P-selectin, results in the formation of growing clusters of adherent cells.

mechanical hypothesis and the seed and soil hypothesis have common elements related to extravasation and colonization, both of which are dependent on the local microenvironment.

As described above, it is likely that there is an optimal range of shear stress, corresponding to values found in the venous system, to achieve a sufficiently long residence time. For example, *in vitro* adhesion assays reveal that metastatic tumour cells bind to the vascular endothelium under venous but not arterial levels of shear stress^{87,93,97}. Furthermore, high shear stresses (12 dyn cm⁻²) similar to those encountered in the arterial circulation have been reported to result in cell cycle arrest of metastatic tumour cells, which facilitates their eradication by the immune system¹¹⁴. By contrast, evidence suggests that low levels of shear stress, typical of the venous system, may have opposite effects on intracellular signalling and tumour cell function. For example, venous shear stress has been suggested to induce an EMT, as shown by the shear-mediated internalization of E-cadherin in metastatic oesophageal OC-1 tumour cells¹¹⁵. Moreover, exposure of free-flowing OC-1 cells to a shear rate of 200 s⁻¹ increased their mobility and invasive capacity *in vitro*¹¹⁵. However, further studies are needed to establish whether these observations can be extended beyond the OC-1 tumour cell line, and whether fluid shear stress can increase the invasive potential of tumour cells *in vivo*.

Conclusions

The physical interactions of cancer cells with the diverse microenvironments encountered during the metastatic process have a key role in the spread of cancer. Mechanical forces modulate cell motility in the architecturally complex extracellular matrix during invasion and in the vascular system during intra-vasation and extravasation. Shear flow in the vascular system dictates the trajectory of circulating tumour cells and has a role in regulating adhesion at blood vessel walls, a key step in extravasation. The emerging insight into the role of physical and mechanical processes in metastasis should contribute to the development of new approaches for cancer diagnosis and treatment. For instance, it is noteworthy that several drug candidates show potential when examined *in vitro* but fail in clinical trials. This failure may stem at least in part from the use of conventional *in vitro* systems that fail to replicate the physiological microenvironment in humans as well as the lack of cell-phenotypic measurements. Specifically, the effects of key

microenvironmental physical properties on cancer and stromal cell responses to drug candidates have yet to be explored in a systematic fashion. These physical properties include mechanical forces, ECM stiffness and the ECM pore size and tortuosity. Moreover, current cutting-edge ‘omic’ measurements conducted on patient specimens need to be complemented with state-of-the-art physical measurements of, for example, cell and tissue microrheology, cell and nuclear shape and cell–cell and cell–matrix adhesion (TABLE 1). Such a holistic approach could drastically reduce the divergent effects of potential drug candidates on cell responses in animal models and in patients, and could help us to identify the appropriate and efficacious targets for treatment.

The authors are at the Departments of Materials Science and Engineering, Chemical and Biomolecular Engineering and Oncology, the Institute for Nanobiotechnology, Johns Hopkins Center of Cancer Nanotechnology Excellence, Johns Hopkins Physical Sciences in Oncology Center, Johns Hopkins University, 3400 North Charles Street, Baltimore, Maryland 21218, USA. e-mails: wirtz@jhu.edu; kk@jhu.edu; searson@jhu.edu
doi:10.1038/nrc3080

1. Chambers, A. F., Groom, A. C. & MacDonald, I. C. Dissemination and growth of cancer cells in metastatic sites. *Nature Rev. Cancer* **2**, 563–572 (2002).
2. Steeg, P. S. Tumor metastasis: mechanistic insights and clinical challenges. *Nature Med.* **12**, 895–904 (2006).
3. Kalluri, R. & Weinberg, R. A. The basics of epithelial-mesenchymal transition. *J. Clin. Invest.* **119**, 1420–1428 (2009).
4. Chaffer, C. L. & Weinberg, R. A. A perspective on cancer cell metastasis. *Science* **331**, 1559–1564 (2011).
5. Thiery, J. P. & Sleeman, J. P. Complex networks orchestrate epithelial-mesenchymal transitions. *Nature Rev. Mol. Cell Biol.* **7**, 131–142 (2006).
6. Polyak, K. & Weinberg, R. A. Transitions between epithelial and mesenchymal states: acquisition of malignant and stem cell traits. *Nature Rev. Cancer* **9**, 265–273 (2009).
7. Hotary, K., Li, X. Y., Allen, E., Stevens, S. L. & Weiss, S. J. A cancer cell metalloprotease triad regulates the basement membrane transmigration program. *Genes Dev.* **20**, 2673–2686 (2006).
8. Hotary, K. B., Allen, E. D., Brooks, P. C., Datta, N. S., Long, M. W. & Weiss, S. J. Membrane type I matrix metalloproteinase usurps tumor growth control imposed by the three-dimensional extracellular matrix. *Cell* **114**, 33–45 (2003).
9. Levental, K. R. *et al.* Matrix crosslinking forces tumor progression by enhancing integrin signaling. *Cell* **139**, 891–906 (2009).
10. De Wever, O., Demetter, P., Mareel, M. & Bracke, M. Stromal myofibroblasts are drivers of invasive cancer growth. *Int. J. Cancer* **123**, 2229–2238 (2008).
11. Provenzano, P. P., Inman, D. R., Eliceiri, K. W. & Keely, P. J. Matrix density-induced mechanoregulation of breast cell phenotype, signaling and gene expression through a FAK-ERK linkage. *Oncogene* **28**, 4326–4343 (2009).
12. Ridley, A. J. *et al.* Cell migration: integrating signals from front to back. *Science* **302**, 1704–1709 (2003).
13. Pollard, T. D. & Borisov, G. G. Cellular motility driven by assembly and disassembly of actin filaments. *Cell* **112**, 453–465 (2003).
14. Lauffenburger, D. A. & Horwitz, A. F. Cell migration: a physically integrated molecular process. *Cell* **84**, 359–369 (1996).
15. Sabeh, F., Shimizu-Hirota, R. & Weiss, S. J. Protease-dependent versus -independent cancer cell invasion programs: three-dimensional amoeboid movement revisited. *J. Cell Biol.* **185**, 11–19 (2009).

16. Fraley, S. I. *et al.* A distinctive role for focal adhesion proteins in three-dimensional cell motility. *Nature Cell Biol.* **12**, 598–604 (2010).
17. Zaman, M. H. *et al.* Migration of tumor cells in 3D matrices is governed by matrix stiffness along with cell-matrix adhesion and proteolysis. *Proc. Natl Acad. Sci. USA* **103**, 10889–10894 (2006).
18. Wozniak, M. A., Desai, R., Solski, P. A., Der, C. J. & Keely, P. J. ROCK-generated contractility regulates breast epithelial cell differentiation in response to the physical properties of a three-dimensional collagen matrix. *J. Cell Biol.* **163**, 583–595 (2003).
19. Yamazaki, D., Kurisu, S. & Takenawa, T. Involvement of Rac and Rho signaling in cancer cell motility in 3D substrates. *Oncogene* **28**, 1570–1583 (2009).
20. Doyle, A. D., Wang, F. W., Matsumoto, K. & Yamada, K. M. One-dimensional topography underlies three-dimensional fibrillar cell migration. *J. Cell Biol.* **184**, 481–490 (2009).
21. Geiger, B., Spatz, J. P. & Bershadsky, A. D. Environmental sensing through focal adhesions. *Nature Rev. Mol. Cell Biol.* **10**, 21–33 (2009).
22. Wehrle-Haller, B. & Imhof, B. The inner lives of focal adhesions. *Trends Cell Biol.* **12**, 382–389 (2002).
23. Parsons, J. T., Horwitz, A. R. & Schwartz, M. A. Cell adhesion: integrating cytoskeletal dynamics and cellular tension. *Nature Rev. Mol. Cell Biol.* **11**, 633–643 (2010).
24. Smith, M. L. *et al.* Force-induced unfolding of fibronectin in the extracellular matrix of living cells. *PLoS Biol.* **5**, e268 (2007).
25. Sun, S. X., Walcott, S. & Wolgemuth, C. W. Cytoskeletal cross-linking and bundling in motor-independent contraction. *Curr. Biol.* **20**, R649–R654 (2010).
26. Bloom, R. J., George, J. P., Celedon, A., Sun, S. X. & Wirtz, D. Mapping local matrix remodeling induced by a migrating tumor cell using three-dimensional multiple-particle tracking. *Biophys. J.* **95**, 4077–4088 (2008).
27. Shih, W. T. & Yamada, S. Myosin IIA dependent retrograde flow drives 3D cell migration. *Biophys. J.* **98**, L29–L31 (2010).
28. Beningo, K. A., Dembo, M., Kaverina, I., Small, J. V. & Wang, Y. L. Nascent focal adhesions are responsible for the generation of strong propulsive forces in migrating fibroblasts. *J. Cell Biol.* **153**, 881–888 (2001).
29. Legant, W. R., Miller, J. S., Blakely, B. L., Cohen, D. M., Genin, G. M. & Chen, C. S. Measurement of mechanical tractions exerted by cells in three-dimensional matrices. *Nature Methods* **7**, 969–971 (2010).
30. Ellsmere, J. C., Khanna, R. A. & Lee, J. M. Mechanical loading of bovine pericardium accelerates enzymatic degradation. *Biomaterials* **20**, 1143–1150 (1999).
31. Beerling, E., Ritsma, L., Vrisekoop, N., Derksen, P. W. & van Rheeenen, J. Intravital microscopy: new insights into metastasis of tumors. *J. Cell Sci.* **124**, 299–310 (2011).
32. Sahai, E., Wyckoff, J., Philippart, U., Segall, J. E., Gertler, F. & Condeelis, J. Simultaneous imaging of GFP, CFP and collagen in tumors *in vivo* using multiphoton microscopy. *BMC Biotechnol.* **5**, 14 (2005).
33. Giampieri, S. *et al.* Localized and reversible TGF-β signalling switches breast cancer cells from cohesive to single cell motility. *Nature Cell Biol.* **11**, 1287–1296 (2009).
34. Hidalgo-Carcedo, C. *et al.* Collective cell migration requires suppression of actomyosin at cell-cell contacts mediated by DDR1 and the cell polarity regulators Par3 and Par6. *Nature Cell Biol.* **13**, 49–58 (2011).
35. Kurisu, S. & Takenawa, T. WASP and WAVE family proteins: friends or foes in cancer invasion? *Cancer Sci.* **101**, 2093–2104 (2010).
36. Iwaya, K., Norio, K. & Mukai, K. Coexpression of Arp2 and WAVE2 predicts poor outcome in invasive breast carcinoma. *Mod. Pathol.* **20**, 339–343 (2007).
37. Yoder, B. J. *et al.* The expression of fascin, an actin-bundling motility protein, correlates with hormone receptor-negative breast cancer and a more aggressive clinical course. *Clin. Cancer Res.* **11**, 186–192 (2005).
38. Li, J. *et al.* PTEN, a putative protein tyrosine phosphatase gene mutated in human brain, breast, and prostate cancer. *Science* **275**, 1943–1947 (1997).
39. Iijima, M. & Devreotes, P. Tumor suppressor PTEN mediates sensing of chemoattractant gradients. *Cell* **109**, 599–610 (2002).
40. Wood, L. D. *et al.* The genomic landscapes of human breast and colorectal cancers. *Science* **318**, 1108–1113 (2007).

41. Sahai, E. & Marshall, C. J. Differing modes of tumour cell invasion have distinct requirements for Rho/ROCK signalling and extracellular proteolysis. *Nature Cell Biol.* **5**, 711–719 (2003).
42. Sounni, N. E. *et al.* MT1-MMP expression promotes tumor growth and angiogenesis through an up-regulation of vascular endothelial growth factor expression. *FASEB J.* **16**, 555–564 (2002).
43. Adhikari, A. S., Chai, J. & Dunn, A. R. Mechanical load induces a 100-fold increase in the rate of collagen proteolysis by MMP-1. *J. Am. Chem. Soc.* **133**, 1686–1689 (2011).
44. Kumar, S. & Weaver, V. Mechanics, malignancy, and metastasis: the force journey of a tumor cell. *Cancer Metastasis Rev.* **28**, 113–127 (2009).
45. Paszek, M. J. *et al.* Tensional homeostasis and the malignant phenotype. *Cancer Cell* **8**, 241–254 (2005).
46. Provenzano, P. P., Inman, D. R., Eliceiri, K. W., Trier, S. M. & Keely, P. J. Contact guidance mediated three-dimensional cell migration is regulated by Rho/ROCK-dependent matrix reorganization. *Biophys. J.* **95**, 5374–5384 (2008).
47. Wirtz, D. Particle-tracking microrheology of living cells: principles and applications. *Annu. Rev. Biophys.* **38**, 301–326 (2009).
48. Friedl, P., Wolf, K. & Lammerding, J. Nuclear mechanics during cell migration. *Curr. Opin. Cell Biol.* **23**, 1–10 (2010).
49. Dahl, K. N., Kahn, S. M., Wilson, K. L. & Discher, D. E. The nuclear envelope lamina network has elasticity and a compressibility limit suggestive of a molecular shock absorber. *J. Cell Sci.* **117**, 4779–4786 (2004).
50. Tseng, Y., Lee, J. S., Kole, T. P., Jiang, I. & Wirtz, D. Micro-organization and visco-elasticity of the interphase nucleus revealed by particle nanotracking. *J. Cell Sci.* **117**, 2159–2167 (2004).
51. Gerlitz, G. & Bustin, M. Efficient cell migration requires global chromatin condensation. *J. Cell Sci.* **123**, 2207–2217 (2010).
52. Crisp, M. *et al.* Coupling of the nucleus and cytoplasm: role of the LINC complex. *J. Cell Biol.* **172**, 41–53 (2006).
53. Stewart-Hutchinson, P. J., Hale, C. M., Wirtz, D. & Hodzic, D. Structural requirements for the assembly of LINC complexes and their function in cellular mechanical stiffness. *Exp. Cell Res.* **314**, 1892–1905 (2008).
54. Hale, C. M. *et al.* Dysfunctional connections between the nucleus and the actin and microtubule networks in laminopathic models. *Biophys. J.* **95**, 5462–5475 (2008).
55. Lee, J. S. *et al.* Nuclear lamin A/C deficiency induces defects in cell mechanics, polarization, and migration. *Biophys. J.* **93**, 2542–2552 (2007).
56. Starr, D. A. & Han, M. ANChors away: an actin based mechanism of nuclear positioning. *J. Cell Sci.* **116**, 211–216 (2003).
57. Starr, D. A. *et al.* unc-83 encodes a novel component of the nuclear envelope and is essential for proper nuclear migration. *Development* **128**, 5039–5050 (2001).
58. Technau, M. & Roth, S. The Drosophila KASH domain proteins Msp-300 and Klaricard and the SUN domain protein klaroid have no essential function during oogenesis. *Fly (Austin)* **2**, 82–91 (2008).
59. Lammerding, J. *et al.* Lamin A/C deficiency causes defective nuclear mechanics and mechanotransduction. *J. Clin. Invest.* **113**, 370–378 (2004).
60. Cross, S. E., Jin, Y. S., Rao, J. & Gimzewski, J. K. Nanomechanical analysis of cells from cancer patients. *Nature Nanotech.* **2**, 780–783 (2007).
61. Guck, J. *et al.* Optical deformability as an inherent cell marker for testing malignant transformation and metastatic competence. *Biophys. J.* **88**, 3689–3698 (2005).
62. Yeung, T. *et al.* Effects of substrate stiffness on cell morphology, cytoskeletal structure, and adhesion. *Cell Motil. Cytoskeleton* **60**, 24–34 (2005).
63. Panorchan, P., Lee, J. S., Kole, T. P., Tseng, Y. & Wirtz, D. Microrheology and ROCK signaling of human endothelial cells embedded in a 3D matrix. *Biophys. J.* **91**, 3499–3507 (2006).
64. Baker, E. L., Bonnecaze, R. T. & Zaman, M. H. Extracellular matrix stiffness and architecture govern intracellular rheology in cancer. *Biophys. J.* **97**, 1013–1021 (2009).
65. Baker, E. L., Lu, J., Yu, D. H., Bonnecaze, R. T. & Zaman, M. H. Cancer cell stiffness: integrated roles of three-dimensional matrix stiffness and transforming potential. *Biophys. J.* **99**, 2048–2057 (2010).
66. Lee, J. S. *et al.* Ballistic intracellular nanorheology reveals ROCK-hard cytoplasmic stiffening response to fluid flow. *J. Cell Sci.* **119**, 1760–1768 (2006).
67. Swartz, M. A. & Fleury, M. E. Interstitial flow and its effects in soft tissues. *Annu. Rev. Biomed. Eng.* **9**, 229–256 (2007).
68. Mycielska, M. E. & Djamgoz, M. B. A. Cellular mechanisms of direct-current electric field effects: galvanotaxis and metastatic disease. *J. Cell Sci.* **117**, 1631–1639 (2004).
69. Fidler, I. J., Yano, S., Zhang, R. D., Fujimaki, T. & Bucana, C. D. The seed and soil hypothesis: vascularisation and brain metastases. *Lancet Oncol.* **3**, 53–57 (2002).
70. Turitto, V. T. Blood viscosity, mass transport, and thrombogenesis. *Prog. Hemost. Thromb.* **6**, 139–177 (1982).
71. Weinbaum, S., Cowin, S. C. & Zeng, Y. A model for the excitation of osteocytes by mechanical loading-induced bone fluid shear stresses. *J. Biomech.* **27**, 339–360 (1994).
72. Weinbaum, S., Duan, Y., Satlin, L. M., Wang, T. & Weinstein, A. M. Mechanotransduction in the renal tubule. *Am. J. Physiol. Renal Physiol.* **299**, F1220–F1236 (2010).
73. Kienast, Y. *et al.* Real-time imaging reveals the single steps of brain metastasis formation. *Nature Med.* **16**, 116–122 (2010).
74. Zhu, C., Yago, T., Lou, J. Z., Zarnitsyna, V. I. & McEver, R. P. Mechanisms for flow-enhanced cell adhesion. *Ann. Biomed. Eng.* **36**, 604–621 (2008).
75. Chang, K. C. & Hammer, D. A. The forward rate of binding of surface-tethered reactants: effect of relative motion between two surfaces. *Biophys. J.* **76**, 1280–1292 (1999).
76. Duguay, D., Foty, R. A. & Steinberg, M. S. Cadherin-mediated cell adhesion and tissue segregation: qualitative and quantitative determinants. *Dev. Biol.* **253**, 309–323 (2003).
77. Niessen, C. M. & Gumbiner, B. M. Cadherin-mediated cell sorting not determined by binding or adhesion specificity. *J. Cell Biol.* **156**, 389–399 (2002).
78. Huang, J. *et al.* The kinetics of two-dimensional TCR and pMHC interactions determine T-cell responsiveness. *Nature* **464**, 932–936 (2010).
79. Marshall, B. T., Long, M., Piper, J. W., Yago, T., McEver, R. P. & Zhu, C. Direct observation of catch bonds involving cell-adhesion molecules. *Nature* **423**, 190–193 (2003).
80. Hynes, R. O. Integrins: bidirectional, allosteric signaling machines. *Cell* **110**, 673–687 (2002).
81. Lorgner, M., Krueger, J. S., O'Neal, M., Staffin, K. & Felding-Habermann, B. Activation of tumor cell integrin $\alpha_5\beta_1$ controls angiogenesis and metastatic growth in the brain. *Proc. Natl Acad. Sci. USA* **106**, 10666–10671 (2009).
82. Gasic, G. J., Gasic, T. B. & Stewart, C. C. Antimetastatic effects associated with platelet reduction. *Proc. Natl Acad. Sci. USA* **61**, 46–52 (1968).
83. Camerer, E. *et al.* Platelets, protease-activated receptors, and fibrinogen in hematogenous metastasis. *Blood* **104**, 397–401 (2004).
84. Karpatic, S., Pearlstein, E., Ambrogio, C. & Coller, B. S. Role of adhesive proteins in platelet tumor interaction *in vitro* and metastasis formation *in vivo*. *J. Clin. Invest.* **81**, 1012–1019 (1988).
85. Nieswandt, B., Hafner, M., Echtenacher, B. & Mannel, D. N. Lysis of tumor cells by natural killer cells in mice is impeded by platelets. *Cancer Res.* **59**, 1295–1300 (1999).
86. Palumbo, J. S. *et al.* Platelets and fibrin(ogen) increase metastatic potential by impeding natural killer cell-mediated elimination of tumor cells. *Blood* **105**, 178–185 (2005).
87. Burdick, M. M. & Konstantopoulos, K. Platelet-induced enhancement of LS174T colon carcinoma and THP-1 monocytoid cell adhesion to vascular endothelium under flow. *Am. J. Physiol. Cell Physiol.* **287**, C539–C547 (2004).
88. Felding-Habermann, B., Habermann, R., Salvador, E. & Ruggeri, Z. M. Role of β_1 integrins in melanoma cell adhesion to activated platelets under flow. *J. Biol. Chem.* **271**, 5892–5900 (1996).
89. Gay, L. J. & Felding-Habermann, B. Contribution of platelets to tumour metastasis. *Nature Rev. Cancer* **11**, 123–134 (2011).
90. Nash, G., Turner, L., Scully, M. & Kakkar, A. Platelets and cancer. *Lancet Oncol.* **3**, 425–430 (2002).
91. Pinedo, H. M., Verheul, H. M., D'Amato, R. J. & Folkman, J. Involvement of platelets in tumour angiogenesis? *Lancet* **352**, 1775–1777 (1998).
92. Crissman, J. D., Hatfield, J., Schaldenbrand, M., Sloane, B. F. & Honn, K. V. Arrest and extravasation of B16 amelanotic melanoma in murine lungs. A light and electron microscopic study. *Lab. Invest.* **53**, 470–478 (1985).
93. Burdick, M. M., McCaffery, J. M., Kim, Y. S., Bochner, B. S. & Konstantopoulos, K. Colon carcinoma cell glycolipids, integrins, and other glycoproteins mediate adhesion to HUVECs under flow. *Am. J. Physiol. Cell Physiol.* **284**, C977–C987 (2003).
94. Borsig, L. *et al.* Heparin and cancer revisited: mechanistic connections involving platelets, P-selectin, carcinoma mucins, and tumor metastasis. *Proc. Natl Acad. Sci. USA* **98**, 3352–3357 (2001).
95. Borsig, L., Wong, R., Hynes, R. O., Varki, N. M. & Varki, A. Synergistic effects of L- and P-selectin in facilitating tumor metastasis can involve non-mucin ligands and implicate leukocytes as enhancers of metastasis. *Proc. Natl Acad. Sci. USA* **99**, 2193–2198 (2002).
96. Jadhav, S., Bochner, B. S. & Konstantopoulos, K. Hydrodynamic shear regulates the kinetics and receptor specificity of polymorphonuclear leukocyte – colon carcinoma cell adhesive interactions. *J. Immunol.* **167**, 5986–5993 (2001).
97. McCarty, O. J. T., Mousa, S. A., Bray, P. F. & Konstantopoulos, K. Immobilized platelets support human colon carcinoma cell tethering, rolling and firm adhesion under dynamic flow conditions. *Blood* **96**, 1789–1797 (2000).
98. Laubli, H., Stevenson, J. L., Varki, A., Varki, N. M. & Borsig, L. L-selectin facilitation of metastasis involves temporal induction of Fut7-dependent ligands at sites of tumor cell arrest. *Cancer Res.* **66**, 1536–1542 (2006).
99. Biancone, L., Araki, M., Araki, K., Vassalli, P. & Stamenkovic, I. Redirection of tumor metastasis by expression of E-selectin *in vivo*. *J. Exp. Med.* **183**, 581–587 (1996).
100. Mannori, G. *et al.* Inhibition of colon carcinoma cell lung colony formation by a soluble form of E-selectin. *Am. J. Pathol.* **151**, 233–243 (1997).
101. Napier, S. L., Healy, Z. R., Schnaar, R. L. & Konstantopoulos, K. Selectin ligand expression regulates the initial vascular interactions of colon carcinoma cells: the roles of CD44v and alternative sialofucosylated selectin ligands. *J. Biol. Chem.* **282**, 3433–3441 (2007).
102. Thomas, S. N., Schnaar, R. L. & Konstantopoulos, K. Podocalyxin-like protein is an E-/L-selectin ligand on colon carcinoma cells: comparative biochemical properties of selectin ligands in host and tumor cells. *Am. J. Physiol. Cell Physiol.* **296**, C505–C513 (2009).
103. Thomas, S. N., Zhu, F., Schnaar, R. L., Alves, C. S. & Konstantopoulos, K. Carcinoembryonic antigen and CD44v cooperate to mediate colon carcinoma cell adhesion to E- and L-selectin in shear flow. *J. Biol. Chem.* **283**, 15647–15655 (2008).
104. Konstantopoulos, K. & Thomas, S. N. Cancer cells in transit: the vascular interactions of tumor cells. *Annu. Rev. Biomed. Eng.* **11**, 177–202 (2009).
105. Varki, A., Varki, N. M. & Borsig, L. Molecular basis of metastasis. *N. Engl. J. Med.* **360**, 1678–1679; author reply 1679–1680 (2009).
106. Jain, S. *et al.* Platelet glycoprotein Iba supports experimental lung metastasis. *Proc. Natl Acad. Sci. USA* **104**, 9024–9028 (2007).
107. Jain, S., Russell, S. & Ware, J. Platelet glycoprotein VI facilitates experimental lung metastasis in syngenic mouse models. *J. Thromb. Haemost.* **7**, 1713–1717 (2009).
108. Weiss, L. Patterns of metastasis. *Cancer Metastasis Rev.* **19**, 281–301 (2000).
109. Jacob, K., Sollier, C. & Jabado, N. Circulating tumor cells: detection, molecular profiling and future prospects. *Expert Rev. Proteomics* **4**, 741–756 (2007).
110. Fidler, I. J. The pathogenesis of cancer metastasis: the 'seed and soil' hypothesis revisited. *Nature Rev. Cancer* **3**, 453–458 (2003).
111. Weiss, L. Comments on hematogenous metastatic patterns in humans as revealed by autopsy. *Clin. Exp. Metastasis* **10**, 191–199 (1992).
112. Paget, S. The distribution of secondary growths in cancer of the breast. *Lancet* **1**, 571–573 (1889).
113. Trepel, M., Arap, W. & Pasqualini, R. *In vivo* phage display and vascular heterogeneity: implications for targeted medicine. *Curr. Opin. Chem. Biol.* **6**, 399–404 (2002).

114. Chang, S. F. *et al.* Tumor cell cycle arrest induced by shear stress: roles of integrins and Smad. *Proc. Natl Acad. Sci. USA* **105**, 3927–3932 (2008).
115. Lawler, K., O'Sullivan, G., Long, A. & Kenny, D. Shear stress induces internalization of E-cadherin and invasiveness in metastatic oesophageal cancer cells by a Src-dependent pathway. *Cancer Sci.* **100**, 1082–1087 (2009).
116. Raub, C. B. *et al.* Noninvasive assessment of collagen gel microstructure and mechanics using multiphoton microscopy. *Biophys. J.* **92**, 2212–2222 (2007).
117. Griffith, L. G. & Swartz, M. A. Capturing complex 3D tissue physiology *in vitro*. *Nature Rev. Mol. Cell Biol.* **7**, 211–224 (2006).
118. Buxboim, A., Ivanovska, I. L. & Discher, D. E. Matrix elasticity, cytoskeletal forces and physics of the nucleus: how deeply do cells 'feel' outside and in? *J. Cell Sci.* **123**, 297–308 (2010).
119. Goldman, A. J., Cox, R. G. & Brenner, H. Slow viscous motion of a sphere parallel to a plane wall — 2 Couette flow. *Chem. Eng. Sci.* **22**, 653–660 (1967).
120. Hanley, W. D., Wirtz, D. & Konstantopoulos, K. Distinct kinetic and mechanical properties govern selectin-leukocyte interactions. *J. Cell Sci.* **117**, 2503–2511 (2004).
121. Panorchan, P. *et al.* Single-molecule analysis of cadherin-mediated cell-cell adhesion. *J. Cell Sci.* **119**, 66–74 (2006).
122. Raman, P., Alves, C., Wirtz, D. & Konstantopoulos, K. Single molecule binding of CD44 to fibrin versus P-selectin predicts their distinct shear-dependent interactions in cancer. *J. Cell Sci.* **124**, 1903–1910 (2011).
123. Li, F., Redick, S. D., Erickson, H. P. & Moy, V. T. Force measurements of the $\alpha 5 \beta 1$ integrin-fibronectin interaction. *Biophys. J.* **84**, 1252–1262 (2003).
124. Bajpai, S. *et al.* α -Catenin mediates initial E-cadherin-dependent cell-cell recognition and subsequent bond strengthening. *Proc. Natl Acad. Sci. USA* **105**, 18331–18336 (2008).
125. Bajpai, S., Feng, Y., Krishnamurthy, R., Longmore, G. D. & Wirtz, D. Loss of α -catenin decreases the strength of single E-cadherin bonds between human cancer cells. *J. Biol. Chem.* **284**, 18252–18259 (2009).
126. Garcia, A. J., Ducheyne, P. & Boettiger, D. Quantification of cell adhesion using a spinning disc device and application to surface-reactive materials. *Biomaterials* **18**, 1091–1098 (1997).
127. DeGrendele, H. C., Kosfizer, M., Estess, P. & Siegelman, M. H. CD44 activation and associated primary adhesion is inducible via T cell receptor stimulation. *J. Immunol.* **159**, 2549–2553 (1997).
128. Palecek, S. P., Loftus, J. C., Ginsberg, M. H., Lauffenburger, D. A. & Horwitz, A. F. Integrin-ligand binding properties govern cell migration speed through cell-substratum adhesiveness. *Nature* **385**, 537–540 (1997).
129. Azioune, A., Storch, M., Bornens, M., Thery, M. & Piel, M. Simple and rapid process for single cell micro-patterning. *Lab. Chip* **9**, 1640–1642 (2009).
130. Thery, M. & Bornens, M. Cell shape and cell division. *Curr. Opin. Cell Biol.* **18**, 648–657 (2006).
131. Khatau, S. B. *et al.* A perinuclear actin cap regulates nuclear shape. *Proc. Natl Acad. Sci. USA* **106**, 19017–19022 (2009).
132. Chen, C. S., Mrksich, M., Huang, S., Whitesides, G. M. & Ingber, D. E. Geometric control of cell life and death. *Science* **276**, 1425–1428 (1997).
133. Mali, P., Wirtz, D. & Searson, P. C. Interplay of RhoA and motility in the programmed spreading of daughter cells postmitosis. *Biophys. J.* **99**, 3526–3534 (2010).
134. Wildt, B., Wirtz, D. & Searson, P. C. Programmed subcellular release for studying the dynamics of cell detachment. *Nature Methods* **6**, 211–213 (2009).
135. Wildt, B., Wirtz, D. & Searson, P. C. Triggering cell detachment from patterned electrode arrays by programmed subcellular release. *Nature Protoc.* **5**, 1273–1280 (2010).
136. Ghaly, T., Wildt, B. E. & Searson, P. C. Electrochemical release of fluorescently labeled thiols from patterned gold surfaces. *Langmuir* **26**, 1420–1423 (2010).
137. Sniadecki, N. J., Lamb, C. M., Liu, Y., Chen, C. S. & Reich, D. H. Magnetic microposts for mechanical stimulation of biological cells: fabrication, characterization, and analysis. *Rev. Sci. Instrum.* **79**, 044302 (2008).
138. Tan, J. L. *et al.* Cells lying on a bed of microneedles: an approach to isolate mechanical force. *Proc. Natl Acad. Sci. USA* **100**, 1484–1489 (2003).
139. Dembo, M. & Wang, Y. L. Stresses at the cell-to-substrate interface during locomotion of fibroblasts. *Biophys. J.* **76**, 2307–2316 (1999).
140. Song, B. *et al.* Application of direct current electric fields to cells and tissues *in vitro* and modulation of wound electric field *in vivo*. *Nature Protoc.* **2**, 1479–1489 (2007).
141. Huang, C. W., Cheng, J. Y., Yen, M. H. & Young, T. H. Electrotaxis of lung cancer cells in a multiple-electric-field chip. *Bioelectron.* **24**, 3510–3516 (2009).
142. Lee, J. S., Chang, M. I., Tseng, Y. & Wirtz, D. Cdc42 mediates nucleus movement and MTOC polarization in Swiss 3T3 fibroblasts under mechanical shear stress. *Mol. Biol. Cell* **16**, 871–880 (2005).
143. Wojciak-Stothard, B. & Ridley, A. J. Shear stress-induced endothelial cell polarization is mediated by Rho and Rac but not Cdc42 or PI 3-kinases. *J. Cell Biol.* **161**, 429–439 (2003).
144. Gomes, E. R., Jani, S. & Gundersen, G. G. Nuclear movement regulated by Cdc42, MRCK, myosin, and actin flow establishes MTOC polarization in migrating cells. *Cell* **121**, 451–463 (2005).
145. Poujade, M. *et al.* Collective migration of an epithelial monolayer in response to a model wound. *Proc. Natl Acad. Sci. USA* **104**, 15988–15993 (2007).
146. Daniels, B. R., Masi, B. C. & Wirtz, D. Probing single-cell micromechanics *in vivo*: the microrheology of *C. elegans* developing embryos. *Biophys. J.* **90**, 4712–4719 (2006).
147. Massiera, G., Van Citters, K. M., Biancianiello, P. L. & Crocker, J. C. Mechanics of single cells: rheology, time dependence, and fluctuations. *Biophys. J.* **93**, 3703–3713 (2007).
148. Solon, J., Levental, I., Sengupta, K., Georges, P. C. & Janmey, P. A. Fibroblast adaptation and stiffness matching to soft elastic substrates. *Biophys. J.* **93**, 4453–4461 (2007).
149. Zhou, X. *et al.* Fibronectin fibrillogenesis regulates three-dimensional neovessel formation. *Genes Dev.* **22**, 1231–1243 (2008).
150. Wang, N., Butler, J. P. & Ingber, D. E. Mechanotransduction across the cell surface and through the cytoskeleton. *Science* **260**, 1124–1127 (1993).
151. Rahman, A., Tseng, Y. & Wirtz, D. Micromechanical coupling between cell surface receptors and RGD peptides. *Biochem. Biophys. Res. Commun.* **296**, 771–778 (2002).
152. Kishino, A. & Yanagida, T. Force measurements by micromanipulation of a single actin filament by glass needles. *Nature* **334**, 74–76 (1988).
153. Zheng, J. *et al.* Tensile regulation of axonal elongation and initiation. *J. Neurosci.* **11**, 1117–1125 (1991).
154. Kumar, S. *et al.* Viscoelastic retraction of single living stress fibers and its impact on cell shape, cytoskeletal organization, and extracellular matrix mechanics. *Biophys. J.* **90**, 3762–3773 (2006).
155. Grill, S. W., Gonczyk, P., Stelzer, E. H. & Hyman, A. A. Polarity controls forces governing asymmetric spindle positioning in the *Caenorhabditis elegans* embryo. *Nature* **409**, 630–633 (2001).
156. Grill, S. W., Howard, J., Schaffer, E., Stelzer, E. H. & Hyman, A. A. The distribution of active force generators controls mitotic spindle position. *Science* **301**, 518–521 (2003).
157. Pajeroski, J. D., Dahl, K. N., Zhong, F. L., Sammak, P. J. & Discher, D. E. Physical plasticity of the nucleus in stem cell differentiation. *Proc. Natl Acad. Sci. USA* **104**, 15619–15624 (2007).
158. Hochmuth, R. M. Micropipette aspiration of living cells. *J. Biomech.* **33**, 15–22 (2000).
159. Lo, C. M., Wang, H. B., Dembo, M. & Wang, Y. L. Cell movement is guided by the rigidity of the substrate. *Biophys. J.* **79**, 144–152 (2000).
160. Engler, A. J., Sen, S., Sweeney, H. L. & Discher, D. E. Matrix elasticity directs stem cell lineage specification. *Cell* **126**, 677–689 (2006).
161. Gerecht, S. *et al.* The effect of actin disrupting agents on contact guidance of human embryonic stem cells. *Biomaterials* **28**, 4068–4077 (2007).
162. Karuri, N. W. *et al.* Biological length scale topography enhances cell-substratum adhesion of human corneal epithelial cells. *J. Cell Sci.* **117**, 3153–3164 (2004).
163. Teixeira, A. I., Abrams, G. A., Bertics, P. J., Murphy, C. J. & Nealey, P. F. Epithelial contact guidance on well-defined micro- and nanostructured substrates. *J. Cell Sci.* **116**, 1881–1892 (2003).
164. Kaspar, D., Seidl, W., Neidlinger-Wilke, C., Ignatius, A. & Claes, L. Dynamic cell stretching increases human osteoblast proliferation and CICP synthesis but decreases osteocalcin synthesis and alkaline phosphatase activity. *J. Biomech.* **33**, 45–51 (2000).
165. Hubbell, J. Biomaterials in tissue engineering. *Biotechnology* **13**, 565–576 (1995).
166. Irimia, D. & Toner, M. Spontaneous migration of cancer cells under conditions of mechanical confinement. *Integr. Biol. (Camb.)* **1**, 506–512 (2009).
167. Wang, C. J. & Levchenko, A. Microfluidics technology for systems biology research. *Methods Mol. Biol.* **500**, 203–219 (2009).
168. Sundararaghavan, H. G., Monteiro, G. A., Firestein, B. L. & Shreiber, D. I. Neurite growth in 3D collagen gels with gradients of mechanical properties. *Biotechnol. Bioeng.* **102**, 632–643 (2009).
169. Quake, S. R. & Scherer, A. From micro- to nanofabrication with soft materials. *Science* **290**, 1536–1540 (2000).
170. Rogers, S. S., Waigh, T. A. & Lu, J. R. Intracellular microrheology of motile *Ameoba proteus*. *Biophys. J.* **94**, 3313–3322 (2008).
171. Condeelis, J. & Segall, J. E. Intravital imaging of cell movement in tumours. *Nature Rev. Cancer* **3**, 921–930 (2003).
172. Kedrin, D. *et al.* Intravital imaging of metastatic behavior through a mammary imaging window. *Nature Methods* **5**, 1019–1021 (2008).
173. Phair, R. D. & Misteli, T. High mobility of proteins in the mammalian cell nucleus. *Nature* **404**, 604–609 (2000).
174. Phair, R. D. & Misteli, T. Kinetic modelling approaches to *in vivo* imaging. *Nature Rev. Mol. Cell Biol.* **2**, 898–907 (2001).
175. Pertz, O. & Hahn, K. M. Designing biosensors for Rho family proteins — deciphering the dynamics of Rho family GTPase activation in living cells. *J. Cell Sci.* **117**, 1313–1318 (2004).
176. Nalbant, P., Hodgson, L., Kraynov, V., Touthckine, A. & Hahn, K. M. Activation of endogenous Cdc42 visualized in living cells. *Science* **305**, 1615–1619 (2004).
177. Moerner, W. E. & Orrit, M. Illuminating single molecules in condensed matter. *Science* **283**, 1670–1676 (1999).
178. Magde, D., Elson, E. L. & Webb, W. W. Fluorescence correlation spectroscopy. II. An experimental realization. *Biopolymers* **13**, 29–61 (1974).
179. Daniels, B. R., Perkins, E. M., Dobrowsky, T. M., Sun, S. X. & Wirtz, D. Asymmetric enrichment of PIE-1 in the *Caenorhabditis elegans* zygote mediated by binary counterdiffusion. *J. Cell Biol.* **184**, 473–479 (2009).
180. Huang, B., Bates, M. & Zhuang, X. Super-resolution fluorescence microscopy. *Annu. Rev. Biochem.* **78**, 993–1016 (2009).
181. Huang, B., Wang, W., Bates, M. & Zhuang, X. Three-dimensional super-resolution imaging by stochastic optical reconstruction microscopy. *Science* **319**, 810–813 (2008).
182. Betzig, E. *et al.* Imaging intracellular fluorescent proteins at nanometer resolution. *Science* **313**, 1642–1645 (2006).

Acknowledgements

The authors gratefully acknowledge support from the US National Institutes of Health (grants U54CA143868, U54CA151838 and RO1CA101135).

Competing interests statement

The authors declare no competing financial interests.

FURTHER INFORMATION

Denis Wirtz's homepage: <http://www.jhu.edu/chembe/wirtz>
 Konstantinos Konstantopoulos's homepage: <http://web1.johnshopkins.edu/kostaslab>
 Peter C. Searson's homepage: <http://www.jhu.edu/searson>
 Johns Hopkins Center of Cancer Nanotechnology Excellence: <http://ccne.inbt.jhu.edu>
 Johns Hopkins Engineering in Oncology Center: <http://psoc.inbt.jhu.edu>

ALL LINKS ARE ACTIVE IN THE ONLINE PDF